



# OPEN Spatial distribution and health risk assessment of fluoride in groundwater in the oasis of the Hotan river basin in Xinjiang, China

Ling Li<sup>1</sup>, Long Ma<sup>2</sup>, Zhilin Pan<sup>2</sup>, Juan Xu<sup>1</sup>, Fei Chen<sup>1</sup>, Changde Yang<sup>1,3</sup>✉ & Yidan Yin<sup>4,5</sup>✉

High fluoride groundwater is a global environmental and public health issue. To explore the effects of fluoride in groundwater in the oasis of the Hotan River Basin in Xinjiang on human health, this study analyzed the content and spatial distribution of fluoride in groundwater. Moreover, health risk assessment was performed using the Monte Carlo method based on the United States Environmental Protection Agency (USEPA) model. The results revealed that the groundwater in the Hotan River Basin oasis has an average  $F^-$  content of  $1.04 \text{ mg} \cdot \text{L}^{-1}$ , with an exceedance rate of 35.2%. High-fluoride groundwater is typically characterized by a high  $\text{HCO}_3^-$  content, low  $\text{Ca}^{2+}$  content relative to  $\text{Mg}^{2+}$  content, and the presence of hydrochemical types of  $\text{Cl} \cdot \text{HCO}_3 \cdot \text{Na}$  and  $\text{HCO}_3 \cdot \text{Na}$ . The hazard quotient (HQ) of fluoride in groundwater  $> 1$  for children and adults in Lop County, Karakax County, and Hotan city and for children in Hotan County. In the study area, the 1–95% quantile certainty of HQ is greater for children (58.30–38.74%) than for adults (52.65–28.26%). Therefore, most residents in the oasis are exposed to the nononcogenic health risks of fluoride in groundwater via the water drinking pathway, with children being highly sensitive. The fluoride content of groundwater in the study area significantly influences the nononcogenic health risk assessment for residents, with a variance contribution rate of 87.8–94.3%. Therefore, reducing the fluoride content in groundwater should be prioritized in decision-making regarding the safety of drinking water in the oasis.

**Keywords** Hydrochemical features, Monte Carlo method, Hazard quotient, Sensitivity analysis

Fluorine is an essential trace element for the human body. Appropriate fluorine intake can promote the healthy development of teeth and bones, but excessive intake can be harmful, potentially causing chronic conditions such as dental fluorosis and skeletal fluorosis<sup>1,2</sup>. Fluorine enters the human body or the food chain via environmental media (water, soil, atmosphere), with drinking water being one of the major exposure pathways<sup>3,4</sup>. In particular, the presence of fluoride (a fluorine-containing compound) in groundwater, a key source of drinking water, is greatly concerning. Compared with surface water, groundwater flows more slowly, which results in prolonged water-rock contact and reaction time<sup>5</sup>. Moreover, groundwater is not rapidly replenished or diluted by atmospheric precipitation<sup>6,7</sup>. As a result, groundwater is more likely to have a high fluoride content. Four globally recognized “fluorination belts” severely affected by high-fluoride groundwater are the East African Rift Valley Belt, West African Mobile Belt, Ancient Mediterranean Active Belt, and Circum-Pacific Volcanic Belt<sup>2,8</sup>. In China, primary high-fluoride groundwater is distributed mainly in northern arid and semiarid areas. Over 60 million people in northwestern China live in areas with a high prevalence of fluorosis, and nearly 20 million patients suffer from fluorosis such as dental fluorosis and skeletal fluorosis nationwide<sup>9</sup>. In these regions, groundwater is often the main or even the only source of water supply. Therefore clarifying the impact of fluoride in groundwater on human health in arid areas is important for engineering safe drinking water<sup>10</sup>.

Health risk assessment is a quantitative description of the risk of adverse health effects caused by human exposure to a certain chemical substance during a certain period of time<sup>11</sup>. The “four-step method” of health risk assessment based on regulations of the National Academy of Sciences (NAS) and United States

<sup>1</sup>Key Laboratory of Xinjiang Coal Resources Green Mining, Ministry of Education, Xinjiang Institute of Engineering, Urumqi 830023, China. <sup>2</sup>Xinjiang Water Conservancy and Hydropower Survey Design Institute CO., LTD, Urumqi 830063, China. <sup>3</sup>School of Mines, China University of Mining and Technology, Xuzhou 221116, China. <sup>4</sup>School of Civil Engineering, Xuchang University, No.88 Bayi Rd, Xuchang 461000, Henan, China. <sup>5</sup>School of Resources and Environment, Xi'an University of Science and Technology, Xi'an 710054, China. ✉email: ycd@cumt.edu.cn; 22209226048@stu.xust.edu.cn

Environmental Protection Agency (USEPA) is widely employed<sup>12,13</sup>. Many countries have developed health risk assessment models applicable to their own countries using the “four-step” evaluation framework as a technical reference<sup>14</sup>. Nevertheless, the selection of model parameters remains the main source of uncertainty in health risk assessment<sup>15</sup>. The model recommended by the USEPA and models recommended by relevant technical guidelines in China mostly involve calculations or evaluations based on the determined concentration of input chemical substances and exposure parameter values, ignoring the unevenness and complexity of the distribution of chemical substances in environmental media as well as individual differences among humans, leading to certain errors in the results<sup>16,17</sup>. To compensate for the shortcomings of uncertainty analysis, the probability method has been widely applied in health risk assessment<sup>18,19</sup>. The probability method follows the same process as the deterministic method does, but the calculation is based on the probability distribution function of the input data and model parameter values rather than a single deterministic value<sup>20</sup>. As in Monte Carlo simulation, random values are repeatedly selected from the probability distribution of each parameter to obtain results expressed in the form of a probability distribution, thereby quantifying uncertainty and improving the accuracy of risk assessment<sup>15,18</sup>. Moreover, sensitivity analysis can also be performed to identify the degree of impact of parameters on risk<sup>21</sup>. The oasis area in the Hotan River Basin is a major population center and an irrigated agricultural area in Xinjiang, where groundwater is the primary source of drinking water<sup>22</sup>. In the 1990 s, to prevent and treat digestive diseases, a drinking water improvement project that replaced surface water with groundwater was carried out in the Hetian area. This led to a problem of fluoride hazards caused by changing the source of drinking water in areas where surface water was originally consumed, resulting in the expansion of fluoride-endemic areas. It also reflected that high fluoride groundwater is the main reason for the high incidence of fluoride toxic diseases in the area<sup>23</sup>. The rural drinking water safety project launched between 2016 and 2020 has significantly improved the quality of drinking water for rural residents in the Hotan area. However, there are still several problems, such as lagging maintenance of water supply facilities, insufficient water treatment technology, and inadequate management systems, which have led to excessive fluoride in drinking water in some areas. According to the *Hotan Groundwater Resource Utilization and Protection Plan* (2022), completed by the Xinjiang Water Conservancy and Hydropower Survey Design Institute Co., Ltd., Hotan city has six water plants, five of which rely on groundwater as the water source; Karakax County has three water plants, two of which rely on both groundwater and surface water, and the third relies solely on groundwater. Drinking water in Hotan County and Lop County is derived from a single water source, that is, groundwater. Extensive research has been conducted on the chemical features and fluoride formation mechanism of high-fluoride groundwater in the Hotan River Basin<sup>24,25</sup>. However, the groundwater samples used in previous studies are outdated and insufficient. Additionally, although recent studies have assessed the health risks of high-fluoride groundwater in the Tarim Basin (including the Hotan River Basin oasis), the health risk assessment results for the Hotan River Basin oasis have not been presented in detail, and the influencing factors have not been identified<sup>26</sup>. Therefore, based on a large amount of sampled data (273 groundwater samples), ArcGIS spatial analysis and the Monte Carlo method were used to explore the fluoride content, spatial distribution, and human health risk in groundwater in the oasis of the Hotan River Basin. This information is highly important for understanding the safety status of drinking water and for preventing and treating fluoride toxicity diseases in the area.

## Study area

The oasis of the Hotan River Basin is located on the alluvial-diluvial plain of the middle reaches of the Hotan River and is distributed along the Yulong Kashi and Karakash rivers (hereinafter referred to as the “two rivers”) (Fig. 1)<sup>28</sup>. It mainly includes four administrative districts: Hotan city, Hotan County, Lop County, and Karakax County. The Hotan River Basin has a warm temperate continental arid desert climate with four distinct seasons and abundant light. The perennial average temperature is 12.2 °C. The region is dry and receives little rainfall, with an average annual precipitation of 35.6 mm and a measured annual evaporation of 2,600 mm<sup>28</sup>.

The hydrogeological conditions of the oasis area are simple<sup>29</sup>. The area has thick Quaternary sediments on the surface, which facilitate the infiltration of surface water. The underlying Paleogene-Neogene strata are composed of sandy, silty, and argillaceous rocks with very low permeability, forming aquicludes. From south to north, aquifers composed of silicate media gradually transition from a single gravel layer to sandy gravel and silty sand layers, and the particles gradually become fine. Moreover, the groundwater hydrodynamic conditions gradually deteriorate along this direction. Taking national highway 315 as the boundary (Fig. 1), the southern region comprises the middle and upper parts of the alluvial-diluvial plain. The hydraulic gradient is 1–4‰ and therefore represents a strong runoff area. The northern region comprises the tail of the alluvial-diluvial plain with a hydraulic gradient of less than 1‰ and therefore represents a weak runoff area.

In general, atmospheric precipitation is not an effective source of groundwater recharge in oasis areas. Rather, groundwater recharge in these areas are primarily derived from the infiltration of water from rivers, canals, and agricultural irrigation, followed by lateral recharge of bedrock fissure water in mountainous areas. The primary groundwater discharge processes include strong surface evaporation and plant transpiration, lateral underground runoff, and artificial exploitation.

## Materials and methods

### Sample collection and testing

From March to May 2022, 273 groundwater samples (all unconfined water samples) were collected from the Hotan River Basin oasis. The distribution of the sampling sites is shown in Fig. 1. The water samples were collected, preserved, and transported in strict accordance with the *Groundwater Sampling Technical Regulations* (DZ/T 0420–2022) and *Technical Regulation of the Preservation and Handling of Samples* (HJ 493–2009). The water samples were analyzed at the laboratory of the First Hydrogeological Engineering Geological Brigade of the Xinjiang Bureau of Geology and Mineral Resources. The tested parameters included Na<sup>+</sup>, Ca<sup>2+</sup>, Mg<sup>2+</sup>, Cl<sup>−</sup>,

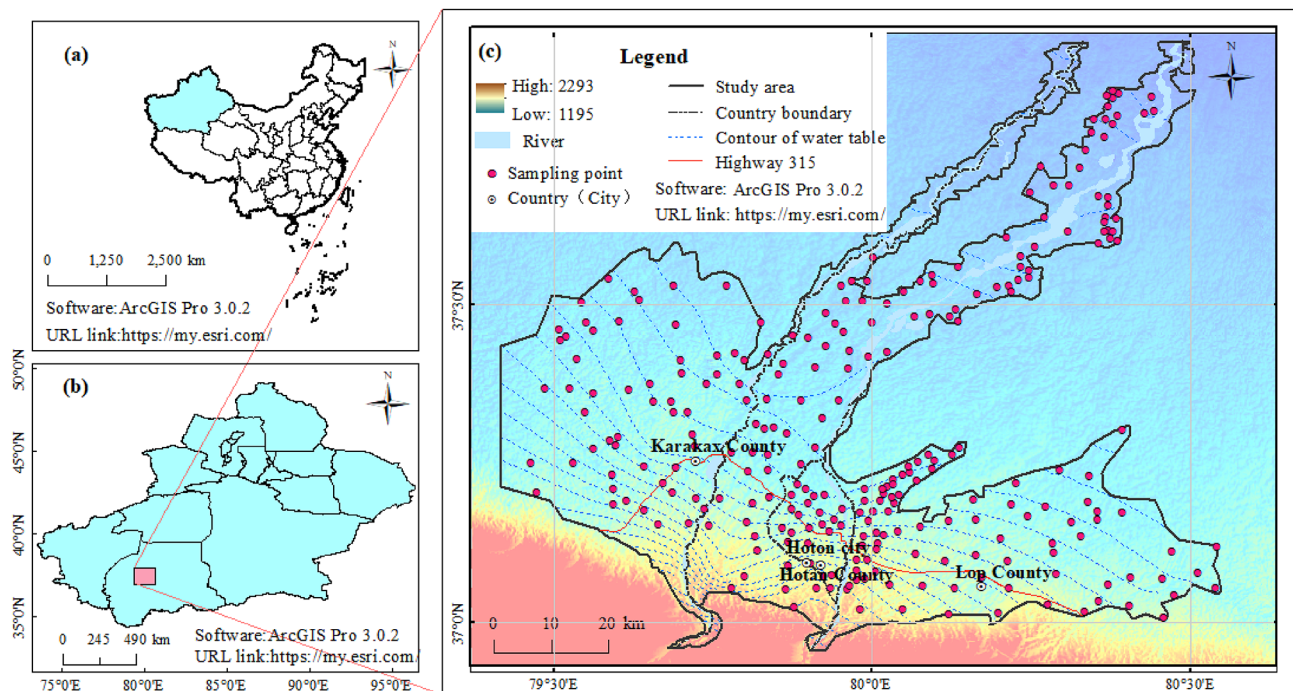


**Fig. 1.** Distribution of the sampling sites<sup>28</sup>.

$\text{SO}_4^{2-}$ ,  $\text{HCO}_3^-$ ,  $\text{CO}_3^{2-}$ ,  $\text{F}^-$ , total dissolved solids (TDS), and pH.  $\text{Na}^+$  was measured using atomic absorption spectrophotometry,  $\text{Ca}^{2+}$  and  $\text{Mg}^{2+}$  were measured via ethylenediaminetetraacetic acid (EDTA) titration,  $\text{Cl}^-$  was measured via silver nitrate titration,  $\text{SO}_4^{2-}$  was measured via barium sulfate turbidimetry,  $\text{HCO}_3^-$  and  $\text{CO}_3^{2-}$  were measured via acid-base titration,  $\text{F}^-$  was measured via the ion-selective, and the detection limits for the above indicators were  $0.1 \text{ mg}\cdot\text{L}^{-1}$ . TDS was performed via gravimetry with a detection limit of  $0.1 \text{ g}\cdot\text{L}^{-1}$ , and the pH was determined via the glass electrode method. The instruments used included an atomic absorption spectrophotometer (Model: WFX-110B, China) and an ionometer (Model: PXSJ-216 F, China). The main chemical reagents used were NaCl (analytical grade), KCl (analytical grade),  $\text{HNO}_3$  (superior grade),  $\text{CsNO}_3$  solution ( $10.0 \text{ g}\cdot\text{L}^{-1}$ ),  $\text{C}_{10}\text{H}_{14}\text{N}_2\text{Na}_2\text{O}_8$  (analytical grade), NaOH (superior grade),  $\text{K}_2\text{CrO}_4$  solution ( $50 \text{ g}\cdot\text{L}^{-1}$ ),  $\text{AgNO}_3$  (analytical grade),  $\text{KAl}(\text{SO}_4)_2\cdot 12\text{H}_2\text{O}$  (analytical grade),  $\text{Na}_2\text{SO}_4$  (analytical grade),  $\text{BaCl}_2$  (analytical grade),  $\text{C}_3\text{H}_8\text{O}_3$  (analytical grade),  $\text{C}_2\text{H}_5\text{OH}$  (analytical grade), phenolphthalein indicator (0.5%), methyl orange indicator (0.1%), NaF (superior grade),  $\text{C}_6\text{H}_5\text{Na}_3\text{O}_7\cdot 2\text{H}_2\text{O}$  (analytical grade), and  $\text{CH}_3\text{COOH}$  (analytical grade), among others. The reliability of the test data was verified using the cation-anion charge balance method, and the error was calculated to be  $\leq \pm 5\%$ .

### Data processing

The groundwater hydrochemical types were classified, and partition maps were drawn. A Piper trilinear diagram was drawn using Origin 2021 from OriginLab to analyze the chemical characteristics of the groundwater. Descriptive statistical analysis was conducted for the groundwater TDS, pH, and  $\text{F}^-$  contents. The spatial distributions of the TDS and  $\text{F}^-$  content of groundwater were plotted using Bayesian kriging interpolation in ArcGIS Pro 3.0.2 from ESRI<sup>27</sup>.

### Methods for health risk assessment

The classification list of carcinogens by the International Agency for Research on Cancer (IARC)<sup>30</sup> and the final assessment list of the toxicity database of the Integrated Risk Information System (IRIS) by the US Environmental Protection Agency (EPA) do not include fluoride as a carcinogen<sup>31</sup>. Therefore, the carcinogenic risk of fluoride was not assessed, and only the nononcogenic health risks of fluoride in groundwater were assessed for adults and children in the oasis using the USEPA model<sup>32</sup>. Considering the main use of groundwater in the study area and the available data, only one exposure pathway—the water drinking pathway—was considered<sup>4</sup>. The assessment model is as follows:

$$HQ = \frac{C \times IR \times ED \times EF}{BW \times AT \times RfD \times WAF} \quad (1)$$

where HQ is the nononcogenic hazard quotient for oral exposure to chemicals in groundwater, which is dimensionless. The meanings of the other parameters are shown in Table 1. If  $HQ > 1$ , then the nononcogenic chemical has negative impacts on human health.

Parameter	Unit	Adult	Children	Probability distribution
Concentration of F <sup>-</sup> in groundwater (C)	mg·L <sup>-1</sup>	Actual measurement	Actual measurement	-
Daily groundwater consumption rate (IR)	L·d <sup>-1</sup>	1.8	0.7	Triangular
Exposure frequency (EF)	d·a <sup>-1</sup>	350	350	Triangular
Exposure duration (ED)	a	24	6	Triangular
Body weight (BW)	kg	56.8	15.9	Normal
Average exposure time (AT)	d	8400	2100	Fixed value
Oral reference dose (RfD)	Mg·(kg·d) <sup>-1</sup>	0.06	0.06	-
Groundwater allocation factor (WAF)	-	0.5	0.5	-

**Table 1.** Exposure parameters in the non-oncogenic health risk assessment model.

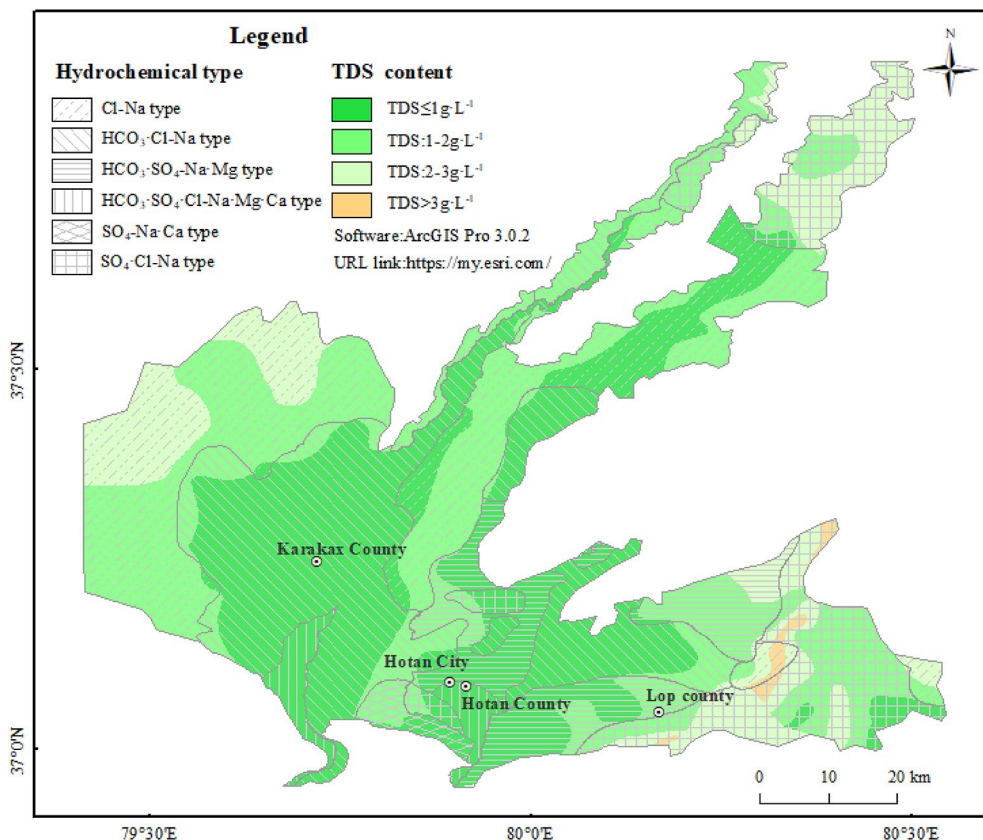


**Fig. 2.** Spatial distribution of fluoride in groundwater<sup>27</sup>.

### Monte Carlo method

Monte Carlo simulation is an effective method for probability and risk analysis. Compared with Bayesian networks and artificial neural networks, this method can significantly reduce uncertainty in health risk assessments, even when the data volume is small<sup>15,18</sup>. In this study, a Monte Carlo simulation was performed using Crystal Ball 11.1.2 from Oracle. The number of iterations was set to 10,000, and the confidence level was 95%<sup>34</sup>. The parameters used in the calculations are shown in Table 1. A sensitivity analysis was also conducted during the simulation process to measure the impact of variable parameters on the health risk assessment<sup>21</sup>.

## Results and discussion

### Hydrochemical features

The pH of groundwater in the Hotan River Basin Oasis ranged from 7.2 to 11.4, with an average of 7.9. Overall, it is weakly alkaline water, with a few cases being strongly alkaline. TDS ranged from 306.2 to 5435.6 mg·L<sup>-1</sup>, with an average of 1315.9 mg·L<sup>-1</sup>, which exceeds the Chinese limit of 1 g·L<sup>-1</sup><sup>35</sup>. The Oasis features six common hydrochemical types of groundwater.

The distribution characteristics of the TDS content and hydrochemical type of groundwater in the Oasis are shown in Fig. 2. As indicated, in the piedmont gravel plain area and along the banks of the Yurungkash River and Karakash River, groundwater is significantly influenced by the infiltration of river water, with deep burial

and good runoff conditions. The TDS content of most samples was  $\leq 1\text{ g}\cdot\text{L}^{-1}$ , with some reaching  $1\text{--}2\text{ g}\cdot\text{L}^{-1}$ . The main hydrochemical types were  $\text{HCO}_3\cdot\text{Cl}\cdot\text{Na}$ ,  $\text{HCO}_3\cdot\text{SO}_4\cdot\text{Na}\cdot\text{Mg}$ , and  $\text{HCO}_3\cdot\text{SO}_4\cdot\text{Cl}\cdot\text{Na}\cdot\text{Mg}\cdot\text{Ca}$ . For instance, groundwater collected near the river valley and piedmont gravel plain area in Karakax County and Hotan County belonged to the types of  $\text{HCO}_3\cdot\text{Cl}\cdot\text{Na}$  and  $\text{HCO}_3\cdot\text{SO}_4\cdot\text{Cl}\cdot\text{Na}\cdot\text{Mg}\cdot\text{Ca}$ , whereas groundwater collected in Qiaerbage Town, Buyaxiang, Lop County and Gujiangbagexiang, Yurungkash Town, Jiyaxiang, and Hotan City belonged to the types of  $\text{HCO}_3\cdot\text{Cl}\cdot\text{Na}$  and  $\text{HCO}_3\cdot\text{SO}_4\cdot\text{Na}\cdot\text{Mg}$ , with the TDS content being  $\leq 1\text{ g}\cdot\text{L}^{-1}$ . Groundwater collected in the area between the Yurungkash River and Karakash River showed various types, including  $\text{Cl}\cdot\text{Na}$ ,  $\text{SO}_4\cdot\text{Cl}\cdot\text{Na}$ ,  $\text{SO}_4\cdot\text{Cl}\cdot\text{Ca}$ ,  $\text{HCO}_3\cdot\text{Cl}\cdot\text{Na}$ , and  $\text{HCO}_3\cdot\text{SO}_4\cdot\text{Na}\cdot\text{Mg}$ , with the TDS content ranging from  $1\text{ to }2\text{ g}\cdot\text{L}^{-1}$ . Further downstream and away from the rivers, the runoff conditions of groundwater worsen, and the groundwater burial depth decreases, resulting in enhanced vertical evaporation and concentration processes. The combination of these factors promotes the accumulation of chemicals in groundwater, resulting in higher TDS, mostly between  $1\text{ and }3\text{ g}\cdot\text{L}^{-1}$ , with low-lying areas exceeding  $10\text{ g}\cdot\text{L}^{-1}$ . The main hydrochemical types of groundwater in these areas are  $\text{Cl}\cdot\text{Na}$  and  $\text{SO}_4\cdot\text{Cl}\cdot\text{Na}$ . For instance, the hydrochemical types of groundwater are  $\text{Cl}\cdot\text{Na}$  at the oasis edge of Karakax County,  $\text{SO}_4\cdot\text{Cl}\cdot\text{Na}$  in Baishituogelakexiang of northern Hangguixiang in Lop County, and  $\text{SO}_4\cdot\text{Cl}\cdot\text{Na}$  within the desert range of northern Hotan County. As indicated, the spatial distribution of groundwater TDS content and hydrochemical types in the oasis area exhibits clear zonation under the influence of climate, topographic features, groundwater recharge and runoff conditions.

Fluoride content

The average  $\text{F}^-$  content in the groundwater of the oasis was  $1.04\text{ mg}\cdot\text{L}^{-1}$ , which exceeded the  $1\text{ mg}\cdot\text{L}^{-1}$  limit, and the exceedance rate was 35.2% (Table 2). The highest  $\text{F}^-$  content ( $4.10\text{ mg}\cdot\text{L}^{-1}$ ) was found in northeast Duoluduoxiang, Lop County. The exceedance rate followed the order of Lop County > Karakax County > Hotan city > Hotan County. In terms of average values, Lop County, Karakax County, and Hotan city all exceeded the standard limit, while only the average fluoride content in groundwater in Hotan County was  $0.83\text{ mg}\cdot\text{L}^{-1}$ , which was lower than the standard limit of  $1\text{ mg}\cdot\text{L}^{-1}$ .

Spatial distribution of fluoride

The spatial distribution of  $\text{F}^-$  in groundwater and its causes were further analyzed by combining the spatial distribution maps of groundwater TDS, hydrochemical types (Fig. 2), and  $\text{F}^-$  content (Fig. 3), as well as the Piper trilinear diagram (Fig. 4) and ion correlation diagram (Fig. 5).

(1) Lop County.

As shown in Fig. 3, the  $\text{F}^-$  content in groundwater in the southwestern part of Lop County near the Yurungkash River and the piedmont gravel plain was generally  $< 1\text{ mg}\cdot\text{L}^{-1}$ . To the east and north of Lop County, which was further from the river and closer to the desert, the groundwater receives less recharge from surface water, the groundwater burial depth decreases, and the runoff weakens, leading to the accumulation of  $\text{F}^-$ .

As shown in Figs. 2 and 3, groundwater with an  $\text{F}^-$  content  $> 3\text{ mg}\cdot\text{L}^{-1}$  was distributed in northeast Duoluduoxiang, and its hydrochemical type was  $\text{SO}_4\cdot\text{Cl}\cdot\text{Na}$  with low  $\text{Ca}^{2+}$  content. Except for at LPX17, the TDS at all the other sites in this area was  $> 2\text{ mg}\cdot\text{L}^{-1}$ . The Piper diagram (Fig. 4) also reveals the same results. Specifically, in groundwater with an  $\text{F}^-$  content of  $> 3\text{ mg}\cdot\text{L}^{-1}$ , the dominant cations were  $\text{Na}^+$  and  $\text{K}^+$ , with a  $\text{Ca}^{2+}$  content  $< 10\%$ , and the dominant anions were  $\text{Cl}^-$  and  $\text{SO}_4^{2-}$ . Compared with groundwater with an  $\text{F}^-$  content exceeding  $3\text{ mg}\cdot\text{L}^{-1}$ , the advantage of  $\text{Na}^+$  in groundwater with an  $\text{F}^-$  content of  $1\text{--}3\text{ mg}\cdot\text{L}^{-1}$  is slightly less. However, the increase in  $\text{HCO}_3^-$  content in most water samples led to a decrease in the dominance of  $\text{Cl}^-$  and  $\text{SO}_4^{2-}$ , and the hydrochemical type was mainly  $\text{HCO}_3\cdot\text{Cl}\cdot\text{Na}$ .

(2) Karakax County.

The  $\text{F}^-$  content in groundwater in Karakax County gradually increased from south to north. In the southern part near the piedmont gravel plain, the  $\text{F}^-$  content in the groundwater was  $< 1.0\text{ mg}\cdot\text{L}^{-1}$ . Along the flow direction of groundwater, the groundwater had a high  $\text{F}^-$  content in some areas. At MYX31, MYX56, and MYX20 near the desert edge, the groundwater  $\text{F}^-$  content  $> 2.0\text{ mg}\cdot\text{L}^{-1}$  (Fig. 3).

As shown in Figs. 3 and 4,  $\text{Na}^+$  was the dominant anion in the groundwater, with an  $\text{F}^-$  content of  $> 2\text{ mg}\cdot\text{L}^{-1}$ , although the dominance was not significant. Additionally, the  $\text{Mg}^{2+}$  content was relatively high, accounting for 30–40%, and the  $\text{Ca}^{2+}$  content was  $< 20\%$ ; the  $\text{HCO}_3^-$  content was approximately 40%, and the  $\text{SO}_4^{2-}$  content was relatively low, accounting for approximately 20%; and the major hydrochemical types were  $\text{HCO}_3\cdot\text{Na}$  and  $\text{Cl}\cdot\text{Na}$ .

(3) Hotan city.

Hotan city is located between the Yurungkash River and the Karakash River, which makes it a strong groundwater runoff zone. However, as shown in Fig. 3, the groundwater in Hotan city had a higher  $\text{F}^-$  content

Location	Mean $\text{mg}\cdot\text{L}^{-1}$	Mix $\text{mg}\cdot\text{L}^{-1}$	Max $\text{mg}\cdot\text{L}^{-1}$	Sample number			
				$\rho(\text{F}^-) \leq 1.0\text{ mg}\cdot\text{L}^{-1}$	$1.0 < \rho(\text{F}^-) \leq 2.0\text{ mg}\cdot\text{L}^{-1}$	$\rho(\text{F}^-) > 2.0\text{ mg}\cdot\text{L}^{-1}$	Over standard rate $\rho(\text{F}^-) \geq 1.0\text{ mg}\cdot\text{L}^{-1}$
Lop County	1.38	0.10	4.10	24	17	10	52.9%
Hotan County	0.83	0.20	3.70	69	17	2	21.6%
Hotan city	1.01	0.10	3.00	52	19	5	31.6%
Karakax County	0.98	0.30	2.50	32	20	6	44.8%
Total	1.04	0.10	4.10	177	73	18	35.2%

Table 2. Statistics of fluoride content in groundwater.

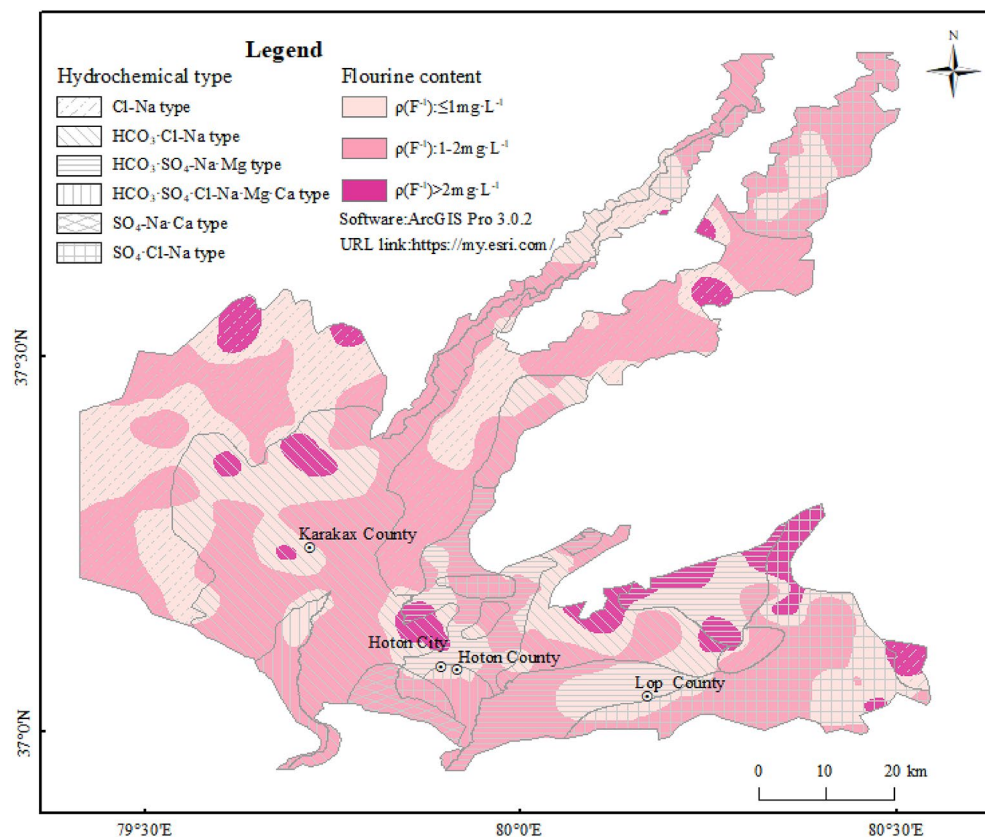


**Fig. 3.** Spatial distribution of fluoride in groundwater<sup>28</sup>.

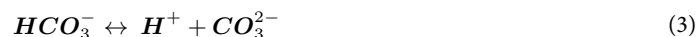
than did the surrounding areas. This may be due to the high population density in Hotan city, as a result of which the  $F^-$  content in groundwater is strongly influenced by human activities<sup>35</sup>.

The distribution of groundwater samples with an  $F^-$  content of  $1-2 \text{ mg} \cdot \text{L}^{-1}$  and  $> 2 \text{ mg} \cdot \text{L}^{-1}$  in the Piper trilinear diagram (Fig. 4) was similar, concentrated mainly in areas where  $\text{Na}^+$  (approximately 50%) was the dominant cation, where the  $\text{Mg}^{2+}$  content (approximately 30%) was higher than the  $\text{Ca}^{2+}$  content (approximately 20%), and where the  $\text{HCO}_3^-$  content was approximately 40%. The hydrochemical types were mainly  $\text{HCO}_3\text{-SO}_4\text{-Na-Mg}$  and  $\text{HCO}_3\text{-Cl-Na}$  (Fig. 3).

#### (4) Hotan County.

Hotan County is located between the Yurungkash River and the Karakash River and extends northward into the desert. As Hotan County is the closest county to the rivers and receives the greatest amount of recharge from the rivers with a low  $F^-$  content, the groundwater of Hotan County has a lower average fluoride content than the other counties do. As shown in Figs. 2 and 3, the excessive groundwater ( $\rho(F^-) > 1 \text{ mg} \cdot \text{L}^{-1}$ ) in Hotan County is mainly of type Cl-Na, dominated by  $\text{Na}^+$  and  $\text{Cl}^-$ .

The hydrochemical characteristics of high-fluoride groundwater ( $\rho(F^-) > 1 \text{ mg} \cdot \text{L}^{-1}$ ) in three counties and one city in the oasis area are similar but also somewhat different. High-fluoride groundwater ( $\rho(F^-) > 1 \text{ mg} \cdot \text{L}^{-1}$ ) is a hydrochemical environment that is favorable for the migration and enrichment of  $F^-$ , with  $\text{Na}^+$  being the dominant cation and  $\text{Mg}^{2+}$  content generally higher than  $\text{Ca}^{2+}$ <sup>37,38</sup>. Research has shown that in arid and semiarid climate zones, due to the lack of aluminum, silicon, and phosphate in groundwater, the fluoride content is controlled by the dissolution equilibrium of calcium-containing minerals such as fluorite ( $\text{CaF}_2$ ) and calcite ( $\text{CaCO}_3$ )<sup>38</sup>. The two will undergo the following reactions in aqueous solution<sup>39</sup>:



If the content of  $\text{HCO}_3^-$  increases, reaction (3) shifts to the right, and reaction (4) shifts to the left, promoting the precipitation of calcite and reducing the activity of  $\text{Ca}^{2+}$  and ultimately leading to an increase in the fluoride content in groundwater<sup>10,40</sup>. There was a significant positive correlation ( $p \leq 0.05$ ) between  $F^-$  and  $\text{HCO}_3^-$  in the groundwater of Lop County (Pearson coefficient of 0.614), Hotan city (Pearson coefficient of 0.506), and

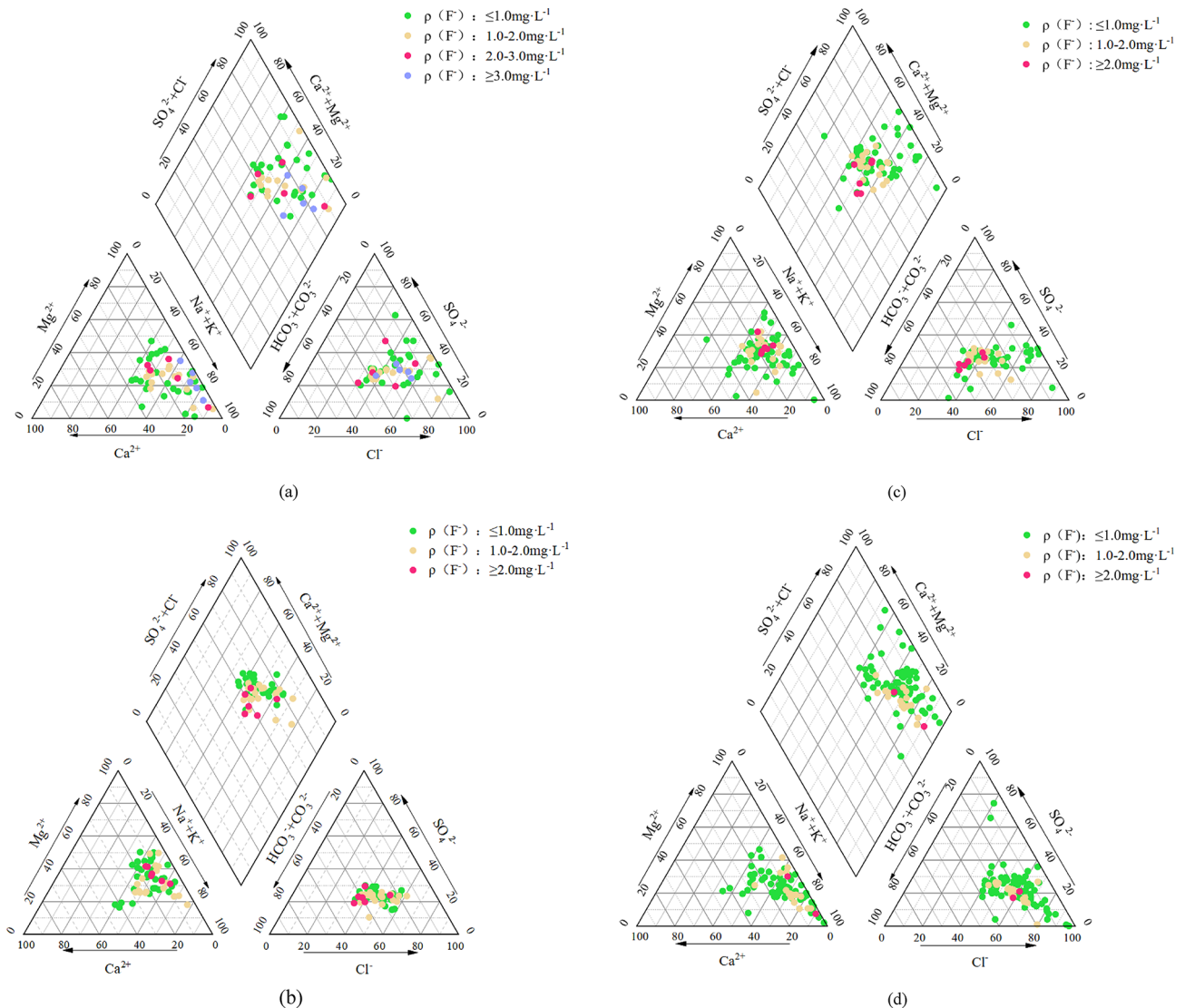


**Fig. 4.** Piper trilinear diagram. **(a)** Lop County; **(b)** Karakax County; **(c)** Hotan city; **(d)** Hotan County.

Karakax County (Pearson coefficient of 0.374) (Fig. 5), and the  $\text{HCO}_3^-$  content reached 40%, indicating that a high  $\text{HCO}_3^-$  content is one of the main factors promoting fluoride enrichment in the groundwater in this area.

The high-fluoride groundwater with a  $\rho(\text{F}^-) > 3 \text{ mg}\cdot\text{L}^{-1}$  in Lop County was dominated by a  $\text{SO}_4^{2-}$  content and a  $\text{HCO}_3^-$  content  $< 40\%$ ; these hydrochemical characteristics inhibit the enrichment of  $\text{F}^-$  in groundwater. However, due to the low  $\text{Ca}^{2+}$  content and proximity to desert areas, this type of groundwater experiences strong evaporation and concentration effects, which also contribute to the accumulation of  $\text{F}^-$ , thus forming high-fluoride groundwater. The characteristics of high-fluoride groundwater in Hotan County also differed, with no significant positive correlation ( $p \leq 0.05$ ) between the  $\text{HCO}_3^-$  and  $\text{F}^-$  contents (Pearson coefficient of 0.257), and the main hydrochemical type was Cl-Na. It can be inferred that the main reason for the enrichment of  $\text{F}^-$  in high-fluoride groundwater in Hotan County is strong evaporation and concentration.

The Gibbs plot (Fig. 6) shows that all water samples fall within the range of evaporation dominance and rock weathering dominance, and no water samples fall within the range of precipitation dominance, especially in the evaporation dominance area, indicating that groundwater is significantly affected by evaporation and concentration. The oasis edges near the deserts in Lop County, Moyu County, and Hotan County are the main distribution areas of high-fluoride groundwater, which also confirms this. Figure 5 shows that groundwater samples with fluoride contents  $< 1.0 \text{ mg}\cdot\text{L}^{-1}$  are more dispersed, whereas groundwater samples with fluoride contents  $> 1.0 \text{ mg}\cdot\text{L}^{-1}$  have  $\text{Na}/(\text{Na} + \text{Ca}) > 0.6$ . This also demonstrates that the high-fluoride groundwater in the oasis is rich in sodium and poor in calcium<sup>41</sup>.

According to the Piper trilinear diagram, groundwater samples with  $\text{F}^-$  contents  $< 1 \text{ mg}\cdot\text{L}^{-1}$  presented a dispersed distribution across the counties and cities. Specifically, some of the samples were distributed in areas overlapping with groundwater samples exceeding the  $\text{F}^-$  limit ( $\rho(\text{F}^-) > 1 \text{ mg}\cdot\text{L}^{-1}$ ), whereas other samples were distributed in areas where neither anions nor cations were dominant. The same findings can be observed from Figs. 2 and 3. The groundwater samples with  $\text{F}^-$  contents  $< 1 \text{ mg}\cdot\text{L}^{-1}$  in the oasis presented low correlations with

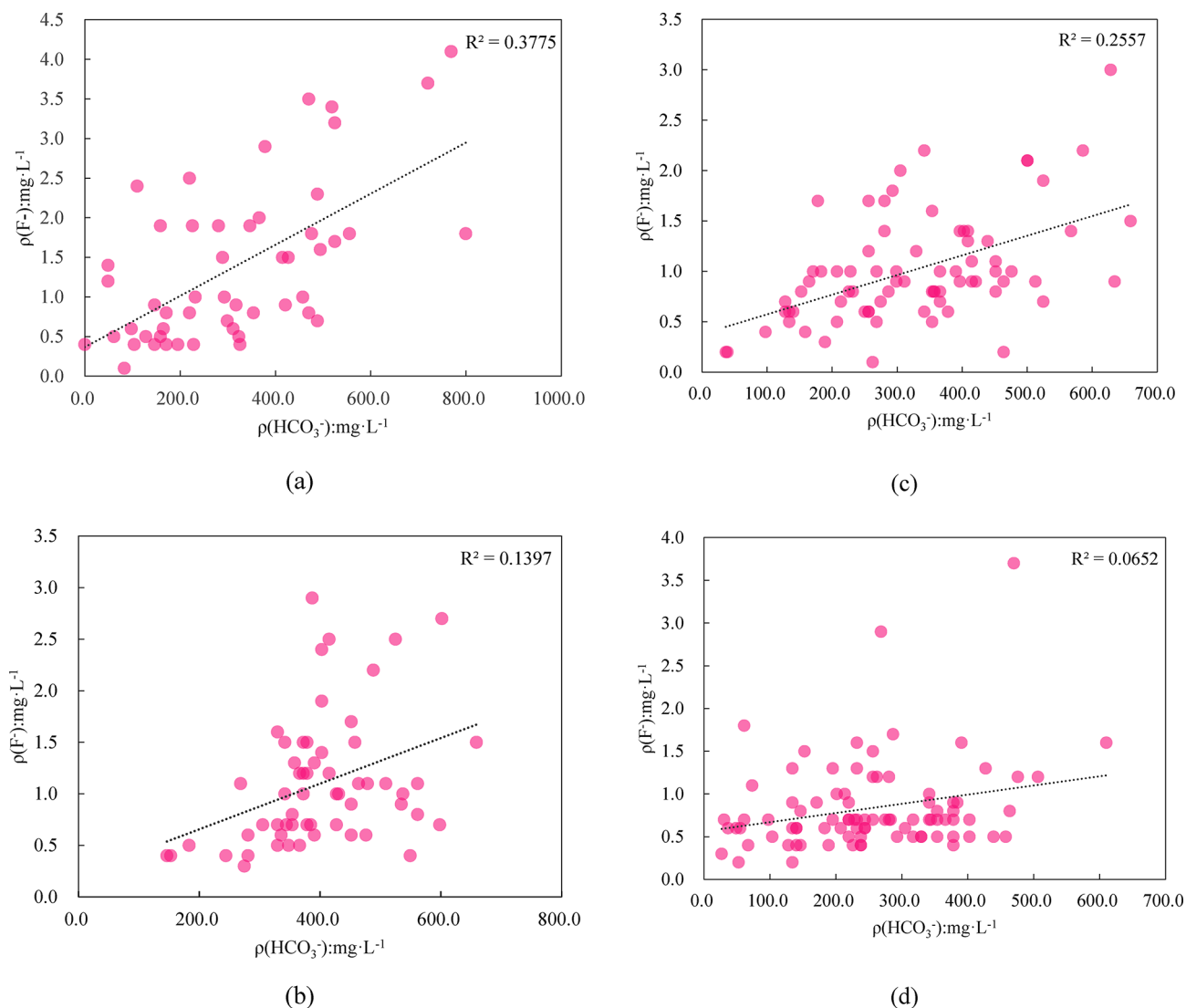


**Fig. 5.** Ionic correlation diagram. (a) Lop County; (b) Karakax County; (c) Hotan city; (d) Hotan County.

the TDS content and hydrochemical type. For example, the  $F^-$  content in groundwater at LSPY19 was  $<0.1 \text{ mg}\cdot\text{L}^{-1}$ , but its TDS exceeded  $3 \text{ g}\cdot\text{L}^{-1}$ . These findings suggest that the factors influencing fluoride migration and accumulation in groundwater in the oasis are very complex.

Overall, under the influences of topographic features, groundwater recharge and runoff conditions, and hydrochemical conditions, the  $F^-$  content in groundwater in the oasis significantly differed among the different sites. The high fluoride groundwater were mainly distributed in areas heavily influenced by human activities, such as Hotan City, and at the oasis edge near the desert in Lop County and Karakax County. The hydrochemical environment with high sodium, low calcium, and high  $\text{HCO}_3^-$  content promoted the enrichment of fluoride in groundwater in oasis areas. In addition, evaporation was also important reasons for the formation of high fluoride groundwater at the edge of oases.

## Health risk assessment

### Probabilistic risk assessment

Based on the distribution characteristics of  $F^-$  content in groundwater and other parameters (Table 1), random numbers were selected by using Oracle Crystal Ball (11.1.2) for the iterative calculation of the non-oncogenic health risk of  $F^-$  in groundwater across the study area according to Formula (1). The specific distribution for each area is as follows: Beta distribution for Hotan City, Log-normal distribution for Hotan County, Gamma distribution for Karakax County, and Log-normal distribution for Lop County. The results are shown in Table 3; Fig. 7.

Fluoride exposure through drinking water poses varying levels of nononcogenic health risks to adults and children in different counties and cities in the Hotan River Basin oasis. The order of HQ for children and adults was Lop County > Karakax County > Hotan city > Hotan County. Except for adults in Hotan County, the mean HQ values exceeded the acceptable risk level recommended by the USEPA for children and adults

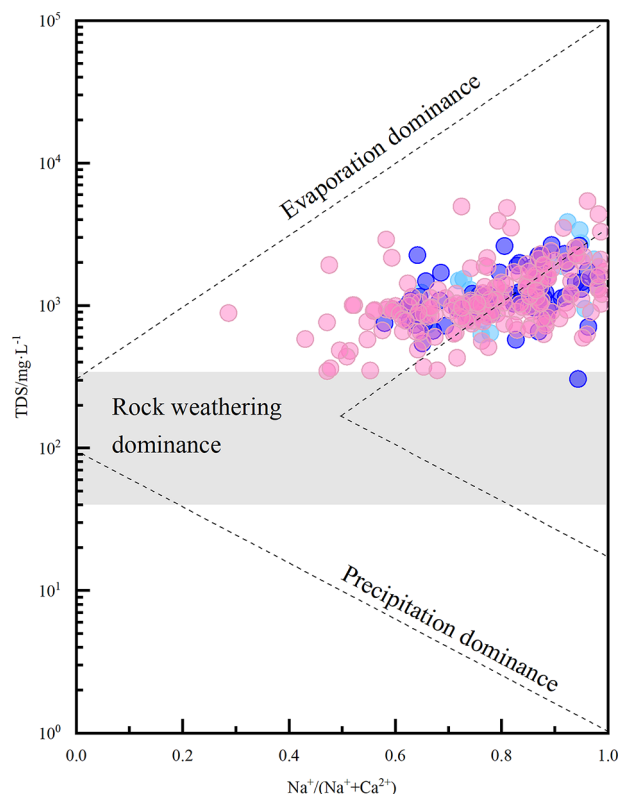


**Fig. 6.** Gibbs plot of groundwater.

Location	Adults		Children	
	Mean	Standard Deviation	Mean	Standard Deviation
Lop County	1.60	1.38	1.83	1.60
Karakax County	1.21	0.76	1.38	0.87
Hotan city	1.13	0.65	1.28	0.75
Hotan County	0.92	0.56	1.05	0.62

**Table 3.** Non carcinogenic HQ of fluoride in groundwater.

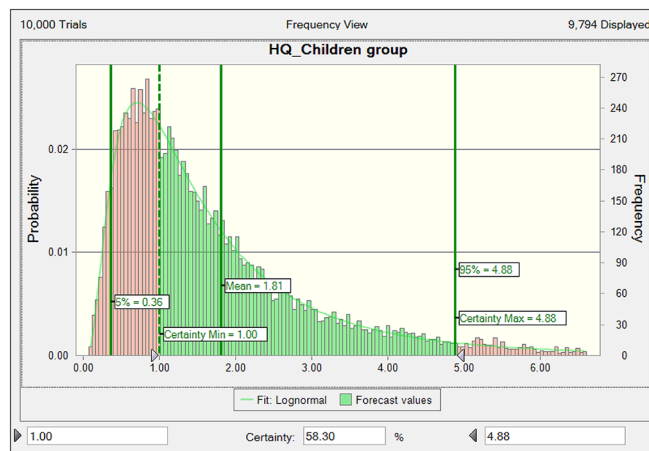
in all other counties and cities. In other words,  $F^-$  in groundwater poses certain nononcogenic health risks to local residents of Lop County, Karakax County, and Hotan city but not to adults in Hotan County. Children are more vulnerable to the harmful effects of  $F^-$  in groundwater than adults are because of their behavioral and physiological characteristics<sup>42,43</sup>. Therefore,  $F^-$  in the oasis groundwater poses greater nononcogenic health risks to children than to adults, suggesting that children are more sensitive to  $F^-$  in groundwater than adults are. This finding is consistent with the findings of previous studies.

According to the probability distribution curve (Fig. 7), the 95% quantile of HQ for children in Lop County was the highest, at 4.83. The certainty of HQ for adults and children across the counties and cities within the 1.0 to 95% quantile range (the blue part of the histogram) varied significantly. In particular, Lop County had the highest certainty at 58.30% for children and 52.65% for adults, whereas Hotan County had the lowest certainty at 38.74% for children and 28.26% for adults. Irrespective of the mean, 95% quantile, or certainty, most residents in the oasis were exposed to nononcogenic health risks from  $F^-$  in groundwater through drinking water. The long-term consumption of such groundwater could significantly increase the risk of fluorosis and other related diseases, with children being the most vulnerable<sup>44,45</sup>.

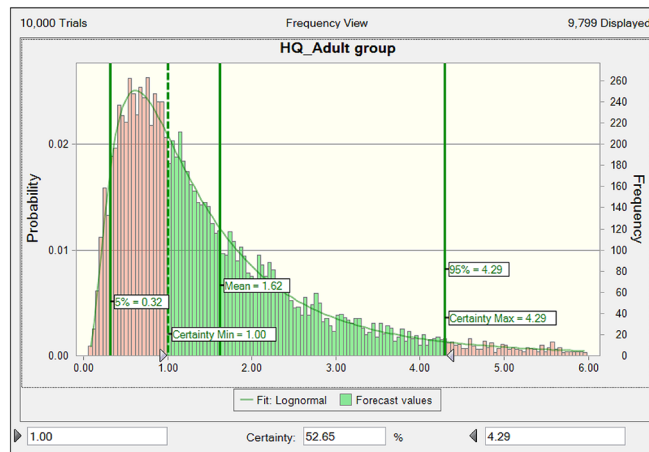
#### Sensitivity analysis

Sensitivity analysis was conducted based on variance, and the variance contribution rate of variable parameters served as a measure of sensitivity. A positive sensitivity value indicates a positive correlation with the risk outcome, whereas a negative sensitivity value indicates a negative correlation. The greater the absolute value of sensitivity, the more significant its impact on the risk outcome<sup>46</sup>.

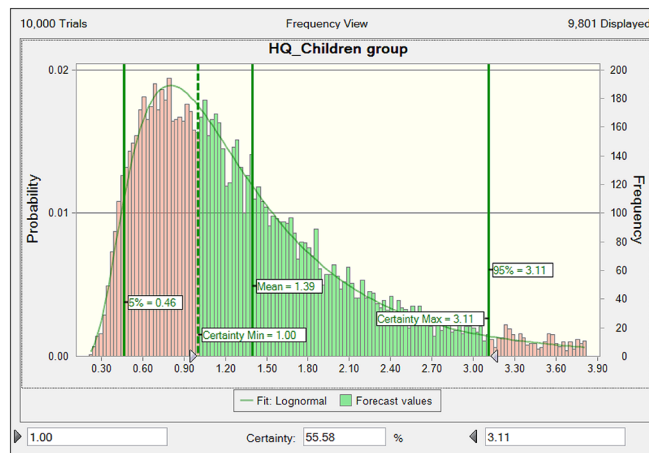
The sensitivities of different counties and cities and different exposure parameters to the nononcogenic health risks of  $F^-$  in groundwater in the study area were plotted (Fig. 8). These findings were consistent with



(a)



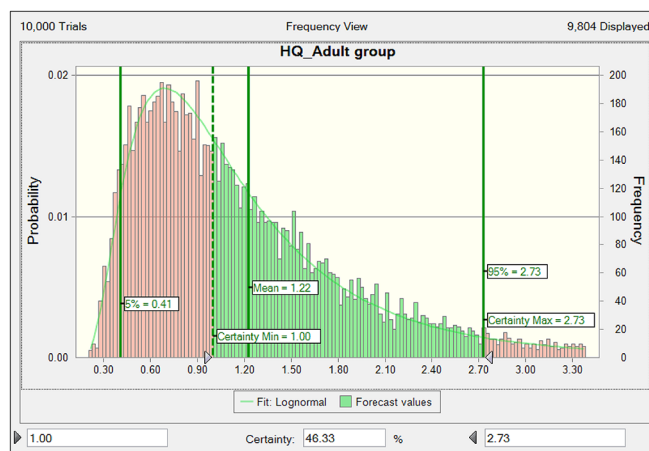
(b)



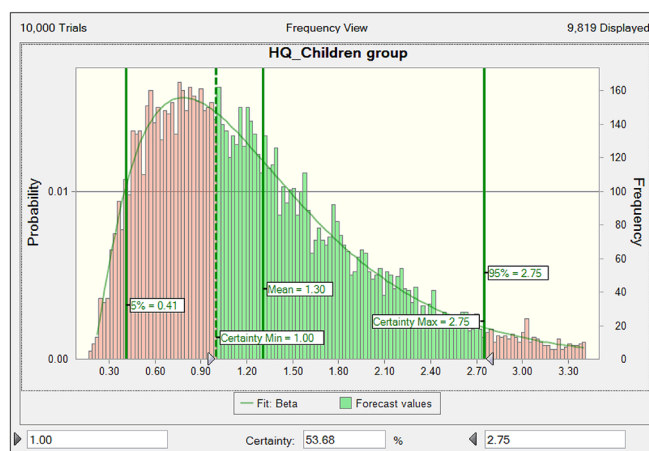
(c)

**Fig. 7.** Histograms of the uncertainty analysis of fluoride HQ. (a) HQ values of the children in Lop County; (b) HQ values of the adults in Lop County; (c) HQ values of the children in Karakax County; (d) HQ values of the adults in Karakax County; (e) HQ values of the children in Hotan city; (f) HQ values of the adults in Hotan city; (g) HQ values of the children in Hotan County; (h) HQ values of the adults in Hotan County.

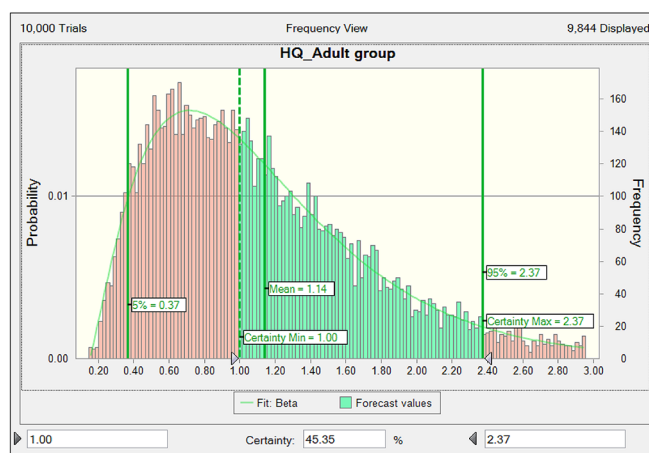
those of previous studies on the effects of  $F^-$  in groundwater on human health in the eastern plains of Xinjiang. Specifically, the fluoride content (C) in groundwater is the most significant factor influencing the nononcogenic health risk assessment for both adults and children in the Hotan River Basin oasis, suggesting a positive sensitivity. For adults, the variance contribution rates of C in Hotan County, Hotan city, Karakax County, and



(d)



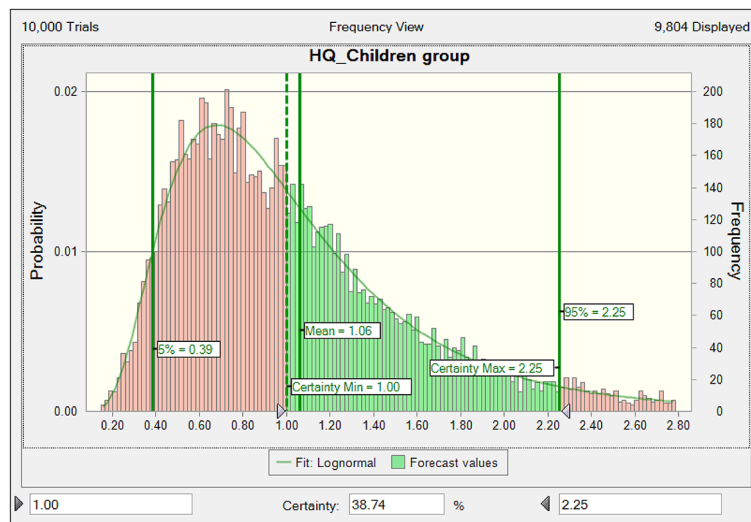
(e)



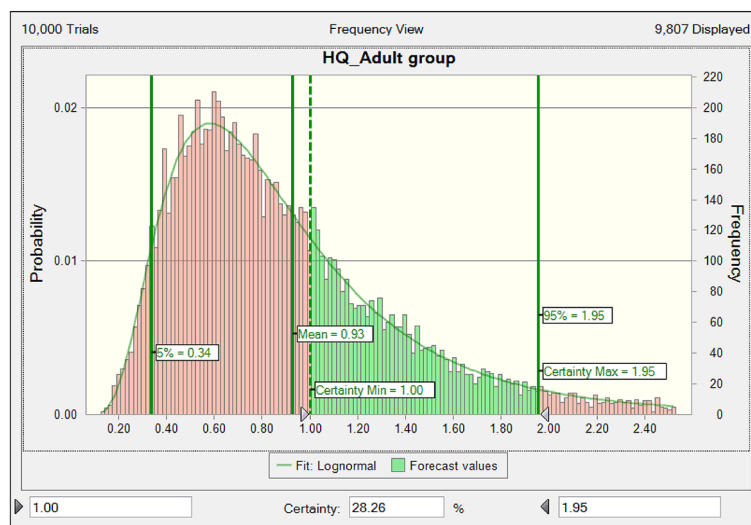
(f)

**Figure 7.** (continued)

Lop County were 87.8, 89.4, 90.2, and 94.0%, respectively. For children, the variance contribution rates were 89.1, 89.8, 90.7, and 94.3%, respectively. This conclusion is consistent with the research of Zeng Y., Ding Q<sup>14,25</sup>. The fluoride content in groundwater directly affects the exposure dose, thereby affecting the HQ value<sup>47</sup>. Fluorine has a low pathogenic threshold for the human body, and even small changes in fluoride levels in groundwater can cause it to exceed these pathogenic thresholds, significantly increasing health risks<sup>48</sup>. In addition to drinking, people also come into contact with fluoride in groundwater through skin contact and other means in their daily lives, further increasing the impact of fluoride content on risk assessment results. As indicated, the larger



(g)



(h)

**Figure 7.** (continued)

the HQ for adults and children in the oasis, the more significant the influence of C was. The order of variance contribution rates of C in the study area was consistent with the order of HQ. Similarly, C had a slightly stronger impact on the nononcogenic health risk assessment for children than for adults. The exposure frequency (EF), exposure duration (ED), and daily average water consumption (IR) were positively correlated with HQ, whereas the average body weight (BW) and average duration of the nononcogenic effect (AT) showed a negative sensitivity. Compared with C, these factors had much weaker influences, with their variance contribution rates all being < 10%<sup>50,51</sup>. Therefore, careful attention should be paid to the safety of drinking water for residents in Karakax County, Lop County, and Hotan city. Moreover, reducing the F<sup>-</sup> content in groundwater is crucial for managing health risks associated with drinking water. The existing measures for artificially controlling the formation of high fluoride groundwater generally have disadvantages such as long operation cycles, insignificant effects, and high cost, which obviously cannot solve the drinking water safety problems in areas where high fluoride groundwater is used as a drinking water source<sup>51</sup>. At the same time, there are no suitable water sources to choose from in the oasis area, and cross regional water transfer has the disadvantage of high economic costs. Therefore, fluoride removal technology needs to be adopted to reduce fluoride in drinking water<sup>52</sup>. To date, not a single technique has been developed that can claim to be a practically robust solution for fluoride removal from drinking water. Therefore, we suggest developing new-generation filters that can retain essential minerals in water and remove only harmful ones and selecting purification technologies according to need, climate, geology, and geographic location<sup>5</sup>.

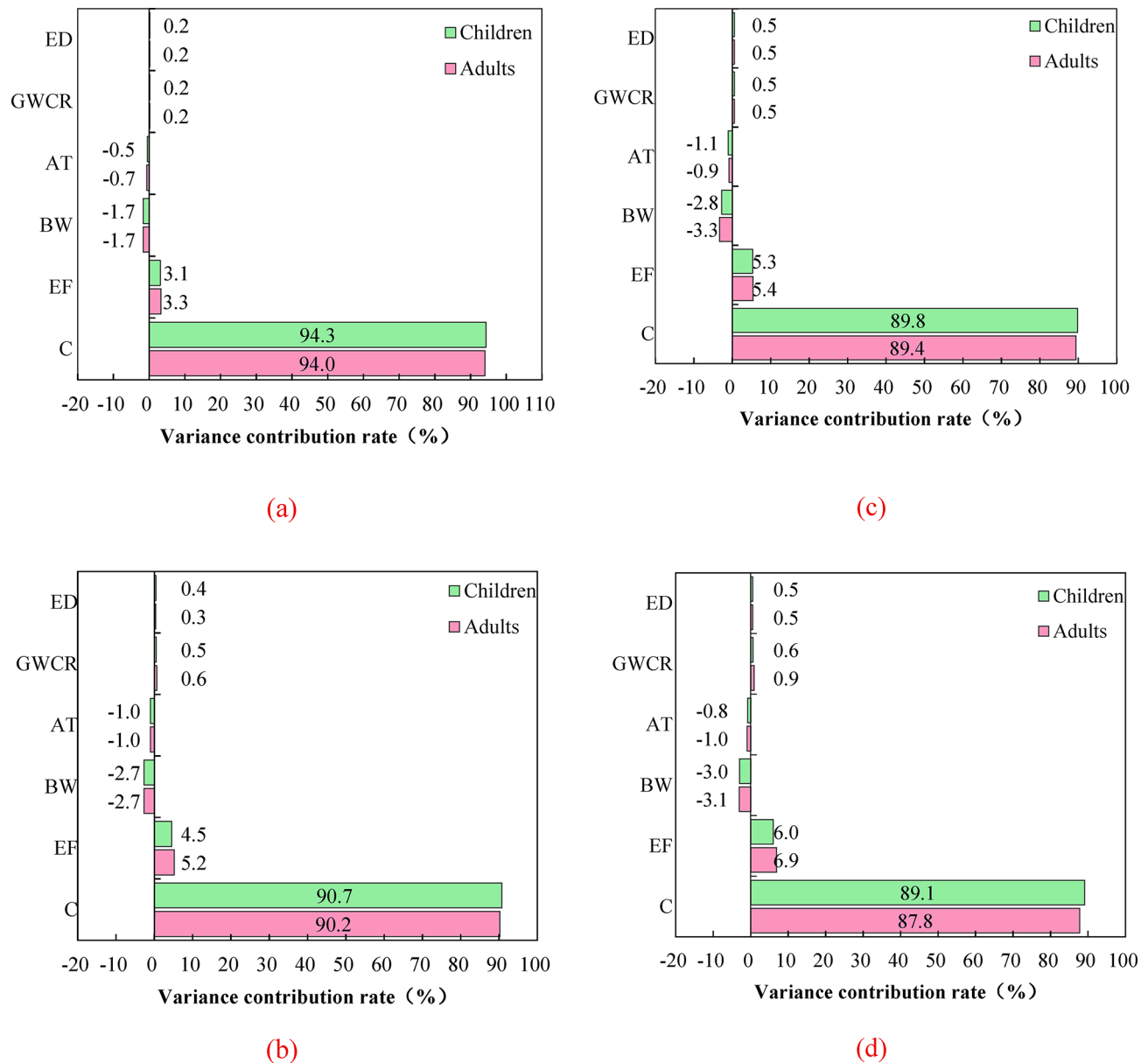


**Fig. 8.** Sensitivity of health risk parameters in adults and children. (a) Lop County; (b) Karakax County; (c) Hotan city; (d) Hotan County.

## Conclusions

(1) The Groundwater in the Hotan River Basin Oasis is weakly alkaline and slightly saline. From areas near the piedmont gravel plain and the river channels to areas downstream and further from the rivers, the TDS of groundwater gradually increased and the major hydrochemical types transitioned from  $\text{HCO}_3\text{-Cl-Na}$ ,  $\text{HCO}_3\text{-SO}_4\text{-Na-Mg}$ , and  $\text{HCO}_3\text{-SO}_4\text{-Cl-Na-Mg-Ca}$  to  $\text{Cl-Na}$  and  $\text{SO}_4\text{-Cl-Na}$ .

(2) The high fluoride groundwater in the oasis area is mainly distributed in the oasis edges near the desert in Lop County and Karakax County, as well as in Hotan City. Overall, the evaporation and hydrochemical environment of high sodium, low calcium, and high  $\text{HCO}_3^-$  content are factors that influence the contamination of groundwater with fluoride.

(3) Most residents in the oasis are exposed to nononcogenic health risks of  $\text{F}^-$  in groundwater, with children being more sensitive than adults. The  $\text{F}^-$  content in groundwater (C) is the most significant factor influencing the nononcogenic health risk assessments of adults and children, exhibiting positive sensitivity. All other factors have a small impact on the assessments. Thus, it is suggested to develop economically feasible, practical and reliable defluorination technologies for high-risk areas, reduce the fluoride content in drinking water, in order to ensure water supply safety.

## Data availability

The datasets used and/or analysed during the current study available from the corresponding author on reasonable request.

Received: 12 November 2024; Accepted: 31 March 2025

Published online: 04 April 2025

## References

- Onipe, T., Edokpayi, J. N. & Odiyo, J. O. A review on the potential sources and health implications of fluoride in groundwater of sub-saharan Africa. *J. Environ. Sci. Health Part. A*. **55** (9), 1078–1093. <https://doi.org/10.1080/10934529.2020.1770516> (2020).
- Wang, Y. et al. Genesis of Geogenic contaminated groundwater: as, F and I. *Crit. Rev. Environ. Sci. Technol.* **51** (24), 2895–2933. <https://doi.org/10.1080/10643389.2020.1807452> (2021).
- Edmunds, W. M. & Smedley, P. L. Fluoride in natural waters. In: (ed Selinus, O.) *Essentials of Medical Geology*. Dordrecht: Springer Netherlands; 311–336. (2013).
- Senthilkumar, M., Mohapatra, B., Gnanasundar, D. & Gupta, S. Identifying fluoride endemic areas and exposure pathways for assessment of non-carcinogenic human health risk associated with groundwater fluoride for Gujarat State, India. *Environ. Sci. Pollut. Res.* **28** (36), 50188–50203. <https://doi.org/10.1007/s11356-021-14156-2> (2021).
- Shaji, E. et al. Fluoride contamination in groundwater: A global review of the status, processes, challenges, and remedial measures. *Geosci. Front.* **15** (2), 101734. <https://doi.org/10.1016/j.gsf.2023.101734> (2024).
- Raza, M., Farooqi, A., Niazi, N. K. & Ahmad, A. Geochemical control on Spatial variability of fluoride concentrations in groundwater from rural areas of Gujrat in Punjab, Pakistan. *Environ. Earth Sci.* **75**, 1–16. <https://doi.org/10.1007/s12665-016-6155-7> (2016).
- Yang, B., Chen, Y., Zhao, C. & Li, Z. Effect of geotextiles with different masses per unit area on water loss and cracking under bottom water loss soil conditions. *Geotext. Geomembr.* **52** (2), 233–240. <https://doi.org/10.1016/j.geotextmem.2023.10.006> (2024).
- Das, S. & Nag, S. K. Geochemical appraisal of fluoride-laden groundwater in Suri I and II blocks, birbhum district, West Bengal. *Appl. Water Sci.* **7** (5), 2559–2570. <https://doi.org/10.1007/s13201-016-0452-x> (2017).
- He, X. et al. Groundwater arsenic and fluoride and associated arsenicosis and fluorosis in China: occurrence, distribution and management. *Expos. Health.* **12** (3), 355–368. <https://doi.org/10.1007/s12403-020-00347-8> (2020).
- Wang, Y. et al. Groundwater quality and health: making the invisible visible. *Environ. Sci. Technol.* **57** (13), 5125–5136. <https://doi.org/10.1021/acs.est.2c08061> (2023).
- Ramesh, R., Subramanian, M., Lakshmanan, E., Subramaniyan, A. & Ganesan, G. Human health risk assessment using Monte Carlo simulations for groundwater with uranium in Southern India. *Ecotoxicol. Environ. Saf.* **226**, 112781. <https://doi.org/10.1016/j.ecoenv.2021.112781> (2021).
- National Research Council. *Risk Assessment in the Federal Government: Managing the Process* (National Academy, 1983).
- U.S. Environmental Protection Agency. Risk assessment guidance for superfund, vol I. Human health evaluation manual (Part A) (Interim Final). Office of Emergency and Remedial Response. Washington, D.C. (1989).
- XIE, H., ZHOU S, LI J, SHEN H, LIN Y, ZHOU C, Z. H. U. D. & WANG Z Spatial distribution, source analysis, and health risk assessment of metal elements in karst water in southeastern Chongqing. *Environ. Sci.* **44** (08), 4304–4313. <https://doi.org/10.13227/j.hjck.202208239> (2023).
- Ding, Q. et al. Spatial distribution, source apportionment and health risk assessment of inorganic pollutant in groundwater in the Eastern plain of Xinjiang. *Earth Sci.* **1–16** doi (2024).
- Ganyaglo, S. Y. et al. Groundwater fluoride contamination and probabilistic health risk assessment in fluoride endemic areas of the upper East region. *Ghana. Chemosphere.* **233**, 862–872. <https://doi.org/10.1016/j.chemosphere.2019.05.276> (2019).
- Morovati, R., Badeenezhad, A., Najafi, M. & Azhdarpoor, A. Investigating the correlation between chemical parameters, risk assessment, and sensitivity analysis of fluoride and nitrate in regional groundwater sources using Monte Carlo. *Environ. Geochem. Health.* **46** (1), 5. <https://doi.org/10.1007/s10653-023-01819-x> (2024).
- Bazeli, J. et al. Health risk assessment techniques to evaluate non-carcinogenic human health risk due to fluoride, nitrite and nitrate using Monte Carlo simulation and sensitivity analysis in groundwater of Khaf County, Iran. *Int. J. Environ. Anal. Chem.* **102** (8), 1793–1813. <https://doi.org/10.1080/03067319.2020.1743280> (2022).
- Padilla-Reyes, D. A. et al. Arsenic and fluoride in groundwater triggering a high risk: probabilistic results using Monte Carlo simulation and species sensitivity distribution. *Chemosphere* **359**, 142305. <https://doi.org/10.1016/j.chemosphere.2024.142305> (2024).
- Kaur, L. et al. Deterministic and probabilistic health risk assessment techniques to evaluate non-carcinogenic human health risk (NHHR) due to fluoride and nitrate in groundwater of Panipat, Haryana, India. *Environ. Pollut.* **259**: 113711.10.1016/j.envpol.2019.113711., 2023. Health risk assessment of heavy metals in agricultural soils around the gangue heap of coal mine based on monte carlo simulation. *Environ. Sci.* **44**(10):5666–5678. doi: 10.13227/j.hjck.202211064. (2020).
- Ling, L. et al. Distribution and formation process of fluorine in groundwater in Oasis area of Hotan river basin. *Arid Land. Resour. Environ.* **33** (1), 112–118 (2019).
- Editorial Committee of Xinjiang Institute of Local Disease Prevention and Control. *Journal of Xinjiang Uyghur Autonomous Region Institute of Local Disease Prevention and Control Urumqi* (Xinjiang People's Health Publishing House, 2008).
- Huang, L., Sun, Z., Zhou, A., Bi, J. & Liu, Y. Source and enrichment mechanism of fluoride in groundwater of the Hotan Oasis within the Tarim basin, Northwestern China. *Environ. Pollut.* **300**, 118962. <https://doi.org/10.1016/j.envpol.2022.118962> (2022).
- Shi, W., Zhou, J., Zeng, Y. & Sun, Y. Distribution characteristics and formation of fluorine in groundwater in Hotan Prefecture. *Arid Zone Res.* **39** (1), 155–164. <https://doi.org/10.13866/j.azr.2022.01.16> (2022).
- Zeng, Y. et al. Enrichment mechanism and health risk assessment of fluoride in groundwater in the Oasis zone of the Tarim basin in Xinjiang, China. *Expos. Health.* **16** (1), 263–278. <https://doi.org/10.1007/s12403-023-00553-0> (2024).
- Luo, M. et al. Multi-model ensemble approaches to assessment of effects of local climate change on water resources of the Hotan river basin in Xinjiang, China. *Water* **9** (8), 584. <https://doi.org/10.3390/w9080584> (2017).
- Esri ArcGIS Pro 3.0.2. Redlands, CA: Esri. (2022). Retrieved from <https://my.esri.com/>
- Feng, F. et al. Hydrogeochemical and statistical analysis of high fluoride groundwater in Northern China. *Environ. Sci. Pollut. Res.* **27** (28), 34840–34861. <https://doi.org/10.1007/s11356-020-09784-z> (2020).
- IARC. Agents classified by the IARC monographs, volumes 1–136. France: International Agency for Research on Cancer; [updated 2024 September 12; accessed 2024 September 26]. (2024). <https://monographs.iarc.who.int/list-of-classifications>
- US Environmental Protection Agency. *IRIS: Integrated Risk Information System* (US Environmental Protection Agency, 2003).
- USEPA. *US Environmental Protection Agency Exposure Factors Handbook* (U.S. Environmental Protection Agency, 1997).
- Zarei, M. R. et al. Non-carcinogenic health risk assessment and Monte Carlo simulation of nitrite, nitrate, and fluoride in drinking water of Yasuj, Iran. *Int. J. Environ. Anal. Chem.* **1–19**. <https://doi.org/10.1080/03067319.2022.2144269> (2022).
- State Administration for Market Regulation of China, Standardization Administration of China. GB 5749–2022: Standards for drinking water quality. Beijing: State Administration for Market Regulation of China and Standardization Administration of China. (2022). <https://www.ndcpa.gov.cn/jbkzxc/c100201/1665979083259711488/hH6H8MSU.pdf>

34. Li, Y., Bi, Y., Mi, W., Xie, S. & Ji, L. Land-use change caused by anthropogenic activities increase fluoride and arsenic pollution in groundwater and human health risk. *J. Hazard. Mater.* **406**, 124337. <https://doi.org/10.1016/j.jhazmat.2020.124337> (2021).
35. Luo, W., Gao, X. & Zhang, X. Geochemical processes controlling the groundwater chemistry and fluoride contamination in the Yuncheng basin, China—An area with complex hydrogeochemical conditions. *PLoS One*. **13** (7), e0199082. <https://doi.org/10.1371/journal.pone.0199082> (2018).
36. Li, J. et al. Hydrogeochemical processes controlling the mobilization and enrichment of fluoride in groundwater of the North China plain. *Sci. Total Environ.* **730**, 138877. <https://doi.org/10.1016/j.scitotenv.2020.138877> (2020).
37. Liang, C., Su, C., Wu, Y. & Li, S. Distribution and geochemical processes for the formation of high fluoride groundwater in Datong basin. *Bull. Geol. Sci. Technol.* **33** (2), 154–159 (2014).
38. Handa, B. K. Geochemistry and genesis of Fluoride-Containing ground waters in India. *Groundwater* **13** (3), 275–281. <https://doi.org/10.1111/j.1745-6584.1975.tb03086.x> (1975).
39. Pazand, K. & Aghavali, N. Hydrogeochemistry of fluoride-enriched groundwater in Khaled-Abad basin, semi-arid region of central Iran. *Appl. Water Sci.* **12** (4), 64. <https://doi.org/10.1007/s13201-022-01597-4> (2022).
40. Gutiérrez, M., Alarcón-Herrera, M. T. & Gaytán-Alarcón, A. P. Arsenic and fluorine in groundwater in Northern Mexico: Spatial distribution and enrichment factors. *Environ. Monit. Assess.* **195** (1), 212. <https://doi.org/10.1007/s10661-022-10818-x> (2023).
41. Wang, S. et al. Identifying the geochemical evolution and controlling factors of the shallow groundwater in a high fluoride area, Feng County, China. *Environ. Sci. Pollut. Res.* **30** (8), 20277–20296. <https://doi.org/10.1007/s11356-022-23516-5> (2022).
42. Amiri, V. & Berndtsson, R. Fluoride occurrence and human health risk from groundwater use at the West Coast of Urmia lake, Iran. *Arab. J. Geosci.* **13** (18), 921. <https://doi.org/10.1007/s12517-020-05905-7> (2020).
43. Qiu, H., Gui, H., Fang, P. & Li, G. Groundwater pollution and human health risk based on Monte Carlo simulation in a typical mining area in Northern Anhui Province, China. *Int. J. Coal Sci. Technol.* **8** (5), 1118–1129. <https://doi.org/10.1007/s40789-021-00446-0> (2021).
44. Ali, S. et al. Health risk assessment due to fluoride exposure from groundwater in rural areas of Agra, India: Monte Carlo simulation. *Int. J. Environ. Sci. Technol.* **18** (11), 3665–3676. <https://doi.org/10.1007/s13762-020-03084-2> (2021).
45. Chen, K. et al. Groundwater pollution source identification and health risk assessment in the North Anhui plain, Eastern China: insights from positive matrix factorization and Monte Carlo simulation. *Sci. Total Environ.* **895**, 165186. <https://doi.org/10.1016/j.scitotenv.2023.165186> (2023).
46. Qiu, H., Gui, H., Xu, H., Cui, L. & Yu, H. Occurrence, controlling factors and noncarcinogenic risk assessment based on Monte Carlo simulation of fluoride in mid-layer groundwater of Huaibei mining area, North China. *Sci. Total Environ.* **856**, 159112. <https://doi.org/10.1016/j.scitotenv.2022.159112> (2023).
47. Li, F. Y. et al. Review on sources of fluorine in the environment and health risk assessment. *Rock. Min. Anal.* **40** (6), 793–807 (2021).
48. Biswas, T., Pal, S. C., Saha, A. & Ruidas, D. Arsenic and fluoride exposure in drinking water caused human health risk in coastal groundwater aquifers. *Environ. Res.* **238**, 117257. <https://doi.org/10.1016/j.envres.2023.117257> (2023).
49. Ali, S. et al. Spatial analysis and probabilistic risk assessment of exposure to fluoride in drinking water using GIS and Monte Carlo simulation. *Environ. Sci. Pollut. Res.* **29** (4), 5881–5890. <https://doi.org/10.1007/s11356-021-16075-8> (2022).
50. Ali, S. et al. Variability of groundwater fluoride and its proportionate risk quantification via Monte Carlo simulation in rural and urban areas of Agra district, India. *Sci. Rep.* **13** (1), 18971. <https://doi.org/10.1038/s41598-023-46197-7> (2023).
51. Song, X., Lu, Y., Liang, S. & Hu, B. Analysis of high-fluoride groundwater formation mechanisms and assessment of health risk in Baxia region. *Zhangjiakou Bull. Geol. Sci. Technol.* **41** (1), 240–250 (2022).
52. Su, G., Liu, G., Huang, Z., Li, Y. & Lin, S. Distribution characteristics and health risk assessment of fluorine in the centralized groundwater drinking water source in Fuyang City. *Environ. Chem.* **43** (10), 3556–3573 (2024).

## Author contributions

Li, L. investigation and supervision. Ma, L., Pan, Z.L. and Xu, J. formal analysis and methodology. Yang, C.D. conceptualization and project administration. Chen, F. and Yin, Y.D. visualization. All authors reviewed the manuscript.

## Funding

This work was supported by the Xinjiang Natural Science Foundation Project “Study on the migration and enrichment mechanism of fluoride in high fluoride groundwater mediated by microorganisms in arid areas(2023D01A84)”, the Xinjiang Institute of Engineering Doctoral Initiation Fund Project “Microbial community, correlation analysis with environmental factors in high fluoride groundwater in arid areas(2024XGYBQJ26)” and the National Natural Science Foundation of China under Grant No.52364021.

## Declarations

## Competing interests

The authors declare no competing interests.

## Additional information

**Correspondence** and requests for materials should be addressed to C.Y. or Y.Y.

**Reprints and permissions information** is available at [www.nature.com/reprints](http://www.nature.com/reprints).

**Publisher's note** Springer Nature remains neutral with regard to jurisdictional claims in published maps and institutional affiliations.

**Open Access** This article is licensed under a Creative Commons Attribution-NonCommercial-NoDerivatives 4.0 International License, which permits any non-commercial use, sharing, distribution and reproduction in any medium or format, as long as you give appropriate credit to the original author(s) and the source, provide a link to the Creative Commons licence, and indicate if you modified the licensed material. You do not have permission under this licence to share adapted material derived from this article or parts of it. The images or other third party material in this article are included in the article's Creative Commons licence, unless indicated otherwise in a credit line to the material. If material is not included in the article's Creative Commons licence and your intended use is not permitted by statutory regulation or exceeds the permitted use, you will need to obtain permission directly from the copyright holder. To view a copy of this licence, visit <http://creativecommons.org/licenses/by-nc-nd/4.0/>.

© The Author(s) 2025